Magneto-Acoustic Emission and Magnetic Barkhausen Emission for Case Depth Measurement in En36 Gear Steel

John W. Wilson[1], Gui Yun Tian[1], Vaidhianathasamy Moorthy[2], and Brian A. Shaw[2]

[1]School of Electrical, Electronic and Computer Engineering, University of Newcastle upon Tyne, Newcastle upon Tyne NE1 7RU, U.K.

[2]Design Unit, School of Mechanical and Systems Engineering, University of Newcastle Upon Tyne, Newcastle Upon Tyne NE1 7RU, U.K.

There is a need in industry to supply safe, economical, and reliable techniques to characterize surface treatments such as case hardening and peening of steel components and structures, both at the manufacturing stage and in service. Magnetic Barkhausen emission (MBE) has proved successful for these tasks, but has severe limitations in terms of measurement depth of the technique and deeper treatments such as laser peening and case hardening often fall outside the scope of MBE inspection. The domain wall motion that generates MBE also causes a release of elastic energy known as magneto-acoustic emission (MAE), which has a much greater measurement depth, and so offers a complementary technique to extend the measurement depth for the characterization of surface treatments in steel. In this paper, comparative MBE and MAE results from case hardened En36 gear steels are presented in the form of signal profiles and correlations are drawn between MBE and MAE profile features and domain activity within the soft core and the case hardened layer. The results show that the overall amplitudes for both MBE and MAE exhibit a good correlation with case depth, but profile analysis for MAE is ambiguous, so possible interpretations of the MAE profile are discussed.

Index Terms—**Case depth, case hardening, En36 steel, magnetic Barkhausen emission, magneto-acoustic emission, nondestructive evaluation, tempering.**

I. Introduction

MAGNETIC BARKHAUSEN EMISSION (MBE) has proven to be a useful and convenient tool in the quantification of microstructural changes and stresses in ferromagnetic materials, but the technique is limited by its low measurement depth. This is especially important for potential industrial applications where measurement depth is a critical factor such as case hardening, which can extend to several millimeters and the quantification of peening treatments, especially laser peening, which can introduce a compressive layer with a depth in excess of 1 mm.

The limiting factor for MBE is the attenuation of the signal source by eddy currents as it propagates through the material, leading to a maximum measurement depth of around 1 mm [1], [2], depending on excitation frequency, analysis frequency range, and material properties. The motion of certain domain configurations (non-180° walls) produce an acoustic pulse, known as magneto-acoustic emission (MAE) [3]–[10], which propagates through the whole test piece unimpeded by eddy currents, thus the measurement depth for MAE is thought to be much greater than for MBE. Consequently, MAE has the potential to provide a complementary inspection technique to MBE both in terms of measurement depth and in terms of differing sensitivities to microstructural configurations.

The benefits of employing a combination of MAE and MBE were first highlighted in the late 1980s by Buttle *et al.* [3], who observed the complementary characteristics of the two techniques in the quantification of heat treatment and stresses in 4360 steel. The authors observed that a combination of MBE and MAE data could be used to first determine the microstructure of the material under inspection and from this information a suitable signal feature could be selected to quantify material stresses, thus reducing the dependence on material specific calibration samples. The effect on both MBE and MAE of work hardening of ferric stainless steels has been studied by O'Sullivan *et al.* [4], where MAE shows a greater correlation to hardening than MBE. The work estimates the maximum measurement depth in ferric stainless steel as 7–8 mm for MAE and 0.1 mm for MBE and as true hardness should be measured through the bulk of the material, this discrepancy in measurement depth is cited as the main cause of the difference in sensitivities of the two techniques. The use of MAE to quantify complex internal stresses on a car leaf spring has been studied by Tochilin *et al.* [5], where MAE measurement depth is controlled by excitation frequency variation and is presumed to correspond to the applied field skin depth, with the maximum measurement depth quoted as 4 mm.

The measurement depth for MAE is often assumed to be proportional to skin depth in a particular material [4], [5], which could potentially equate to several centimeters, but the validity of this assumption is questionable on several levels. First, the validity of the skin depth formula for the low excitation frequencies used for MAE inspection is questionable and the actual field distribution is influenced by other factors such as the geometry of the sample and the intensity of the applied field. Augustyniak *et al.* [6] explain the distribution of the flux in a particular sample in terms of two factors; penetration: the flux reaching the bottom of the sample straight through its thickness and flow around: the flux concentrating in the surface layer of the material en route to the bottom of the sample. The flux within the surface layer can travel far with relatively little attenuation or phase lag, whereas the subsurface regions suffer from increased screening from the induced field. The flow around effect increases with excitation frequency and also increases in narrower samples, re-

Manuscript received July 14, 2008; revised October 06, 2008. Current version published January 30, 2009. Corresponding author: J. W. Wilson (e-mail: john.wilson2@ncl.ac.uk).

Color versions of one or more of the figures in this paper are available online at http://ieeexplore.ieee.org.

Digital Object Identifier 10.1109/TMAG.2008.2007537

ducing the field intensity in subsurface layers. Second, the intensity of the induced field will decrease with depth in almost all samples (a possible exception being samples with a change in permeability with depth), so less MAE activity is expected in subsurface layers and that activity may be masked by surface activity. Third, the propagation characteristics of MAE are not fully understood and are dependant on factors such as sample geometry, material microstructure and sensor characteristics. In order to fully understand the measured MAE signal, all these factors must be taken into account.

This paper summarizes the results of an ongoing investigation into the utilization of a combination of MAE and MBE to provide a case depth measurement system for En36 gear steel. The aim of the project is to extend the current limit of around 1 mm for case depth measurement using MBE to several millimeters using complementary MAE data. MBE and MAE investigation is undertaken using the established signal profile analysis technique [1]–[3] and an attempt is made to correlate signal strength at a particular point in the excitation cycle with the spatial positioning of domain activity within the sample.

Some issues associated with system design and sensor selection are outlined in Section II, an investigation into the characterization of heat treatment in 0.1% carbon steel is presented in Section III, and an investigation into the characterization of case hardening in En36 gear steel is presented in Section IV followed by conclusions in Section V.

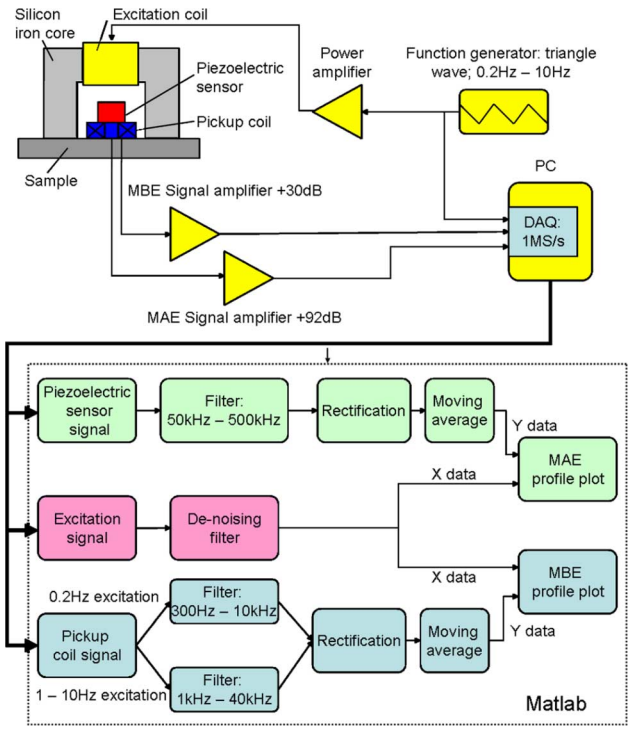

Fig. 1. Block diagram of integrated MBE and MAE system and profile generation process.

II. System Design, Signal Analysis, and Sample Summary

This section details the integrated MAE and MBE system and signal processing techniques developed for the tests and provides a summary of the 0.1% carbon steel and En36 gear steel samples used in the tests.

A. System Design and Signal Analysis

A block diagram of the system used in the tests is shown in Fig. 1. The excitation waveform is provided by a function generator, with the excitation signal routed to a silicon-iron core wrapped with an excitation coil, via a power amplifier. The voltage applied by the function generator is recorded as a reference signal, as it provides an independent parameter which is not influenced by changes in the magnetic properties of the sample as the applied field or excitation current would be. The core is mounted on the sample under inspection with no air gap between the pole faces and the sample. MBE measurements are made using a pickup coil interfaced to a PC data acquisition card via instrumentation amplifier based signal conditioning circuitry. MAE measurements are made using a Physical Acoustics u30 piezoelectric acoustic emission sensor routed to a PC data acquisition card via a Physical Acoustics preamplifier. Data acquisition is performed using LabView at a rate of 1 MS/s per channel, with signal processing performed in Matlab. Software filtering is used to separate the MBE signal from the low-frequency envelope. Although this does decrease the achievable signal-to-noise ratio for the MBE signal, it does allow greater flexibility for signal analysis.

The pickup coil used in the tests is wound around a 2 mm ferrite core and potted in a 22 mm diameter, 18 mm high cylindrical aluminium case, which provides some shielding from direct fields from the excitation core. The coil has a resistance of 5.2 kHz, inductance of 880 mH, and a resonant frequency of 16.5 kHz. The number of turns in the coil is not known, but is estimated to be in the order of several thousand.

Calculation of MBE and MAE signal profiles is outlined in Fig. 1. Signals corresponding to ten excitation cycles are recorded from the pickup coil and the piezoelectric acoustic emission sensor along with the excitation voltage. The pickup coil signal is filtered to separate the MBE from the low-frequency envelope and the signal from the piezoelectric sensor is filtered to remove any extraneous noise. Both signals are rectified and signal profiles are calculated using a moving average technique. Signal profiles from several excitation cycles are calculated; the results are averaged and plotted against the recorded excitation voltage.

In order to eliminate the low-frequency envelope of the pickup coil signal, an MBE high-pass filter frequency of 1 kHz was chosen for excitation frequencies of 1 Hz and above, with a 300 Hz high-pass filter chosen for 0.2 Hz excitation. As MBE is subject to eddy-current shielding which increases with increasing depth, signal sources from domain activity at a particular depth, propagating through the material to the sensor at the surface are subject to an effect which is analogous to the application of a low-pass filter with cutoff frequency decreasing with increased signal source depth. So measurement is confined to the near-surface layer and only lower frequency sections of the signal contain information from the deeper layers. As eddy-current shielding is governed by the skin depth formula, maximum measurement depth (δ) for a high-pass filter frequency (f) is given by

$$\delta = \frac{1}{\sqrt{f\pi\mu\sigma}} \tag{1}$$

where, for En36 steel, magnetic permeability, $\mu = 4\pi \times 10^{-7} \times 200$ and conductivity, $\sigma = 3.15 \times 10^{6}\ \Omega^{-1}\ \mathrm{m}^{-1}$ [2], giving a maximum measurement depth of around 634 μm for the 1 kHz filter and 1.16 mm for the 300 Hz filter. As MAE is an acoustic signal and therefore not subject to attenuation by eddy currents, the theoretical measurement depth at a frequency of 2 Hz for example, is equal to the skin depth at 14 mm, but at very low frequencies it is doubtful whether this holds true and the actual field distribution is influenced by other factors such as the intensity of the applied magnetic field and sample geometry. The propagation characteristics of the signal, including sound attenuation and reverberation from object boundaries [6] should also be taken into account.

Signal profile analysis allows the intensity of the signal at different points in the excitation cycle to be studied. As Barkhausen activity at different excitation voltages corresponds to different microstructural and magnetic states of the material, the signal profile can be used to draw inferences about different material layers. For example, case hardened steel has a soft core and a hardened surface layer, so Barkhausen activity at low excitation voltages corresponds to activity in the softer core of the material, whereas activity at higher excitation voltages corresponds to activity in the harder surface layer. Although this has been proved to be true for MBE [1], [2], the situation for MAE is slightly different; whereas MBE is measured in a small area in the near surface layer directly below the sensor, a single sensor mounted at the surface of the material can sense all MAE activity induced in the material. As the time/space distribution and intensity of the magnetic flux in the material varies with respect to the position of the excitation apparatus [7], the measured signal corresponds to an integration of activity over a large area with differing phase relationships with the excitation signal.

B. MAE Sensor Selection

Fig. 2 shows signal profiles for two different MAE sensors; a physical acoustics R15 150 kHz resonant sensor with an operating frequency range of 50 kHz–200 kHz and a sensing surface diameter of 15 mm and a u30 300 kHz resonant sensor with an operating frequency range of 100 kHz–400 kHz and a sensing surface diameter of 8 mm. MAE activity is referenced to the excitation voltage, which is shown along the x-axis. The MAE profiles corresponding to the rising half cycle (-2 v to 2 v) and the falling half cycle (2 v to -2 v) are plotted separately on the same axes. It can be seen from the plots that the u30 sensor (Fig. 2(b)) gives a much greater variation for the samples examined in the test. A number of these comparative tests were carried out using different materials, with similar results and the u30 sensor was selected as the most appropriate sensor for the tests.

The u30 probe exhibits better linearity than the R15 probe due to its decreased diameter. At an estimated signal velocity of 3000 m/s in steel, the wavelength equivalent to the surface diameter (8 mm) of the u30 probe corresponds to a frequency of 375 kHz, whereas the wavelength equivalent to the surface diameter (15 mm) of the R15 probe corresponds to a frequency of 200 kHz. Thus, the u30 sensor offers increased spatial resolution and an increased frequency range which provides extra MAE data. From the results shown in Fig. 2 and other test results it is apparent that for the samples used in these tests this increased frequency range carries important information which allows discrimination between samples with differing case depths.

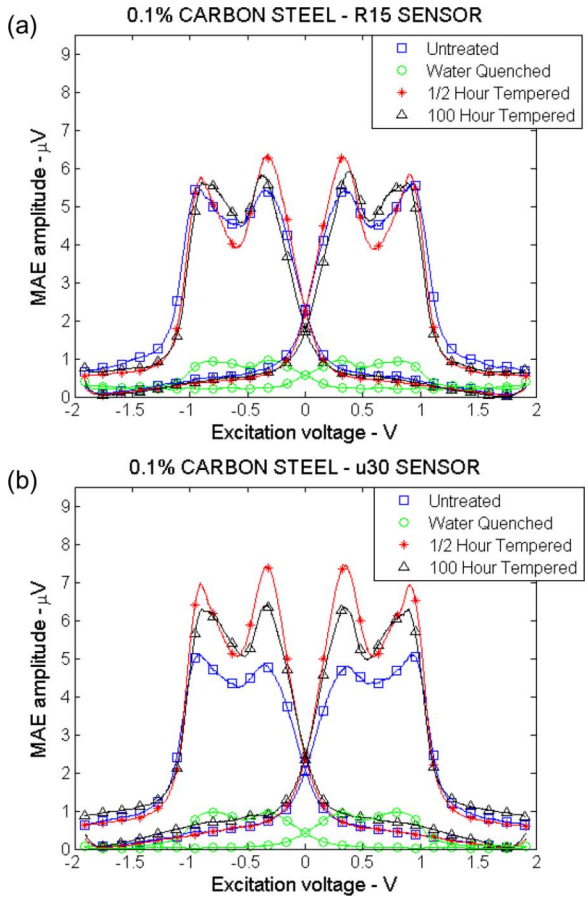

Fig. 2. Typical MAE profiles for R15 (a) and U30 (b) sensors.

C. Sample Summary

Three sets of samples are used in the tests; heat treated 0.1% carbon steel, case hardened En36 steel bars, and case hardened En36 blocks. The characteristics and dimensions of the samples are summarized in Table I, where the case depths are validated by X-ray diffraction techniques.

III. Characterization of Heat Treatment of 0.1% Carbon Steel

In this section, the comparative strengths of MAE and MBE for the characterization of heat treatment in 0.1% carbon steel are studied. This mild steel shows much stronger Barkhausen activity than the harder gear steels and the results are useful to identify signal characteristics which may not be as easily identifiable in the gear steels.

Fig. 3 shows MAE and MBE activity for 650°C heat treated 0.1% carbon steel samples (samples a1–a4) using 2 Hz triangle wave excitation. Several remarks can be drawn from comparison of the plots: first, the water quenched sample does show a distinct reduction in MBE activity, but the shape and peak position of the profile is very similar to the 1/2 hour tempered sample, with reduced amplitude, introducing some ambiguity into the interpretation of the MBE plot, but MAE activity is reduced almost to zero, this indicates that the microstructure is predominantly martensitic, as martensite has only one easy magnetic axis, producing no MAE activity. As the martensitic structure recovers with the application of heat treatment, both MAE and MBE increase, with maximum activity for MAE for the 1/2 hour

TABLE I
SUMMARY OF SAMPLES

Description	Width	Depth	Length
a) 0.1% carbon steel samples with various heat treatments applied			
A1 – As received	12mm	4mm	112mm
A2 – Water quenched	12mm	4mm	94mm
A3 – Tempered for 0.5 hours at 650º c	12mm	4mm	105mm
A4 – Tempered for 100 hours at 650º c	10mm	4mm	110mm
b) Case hardened En36 bar samples			
B1 – Untreated	10mm	10mm	119mm
B2 – 0.65mm case	12mm	10mm	119mm
B3 – 0.75mm case	12mm	10mm	119mm
B4 – 1.00mm case	12mm	10mm	119mm
B5 – 1.35mm case	12mm	10mm	119mm
c) Case hardened En36 block samples			
C1 – 1.00mm case	30mm	10mm	110mm
C2 – 2.00mm case	30mm	10mm	110mm

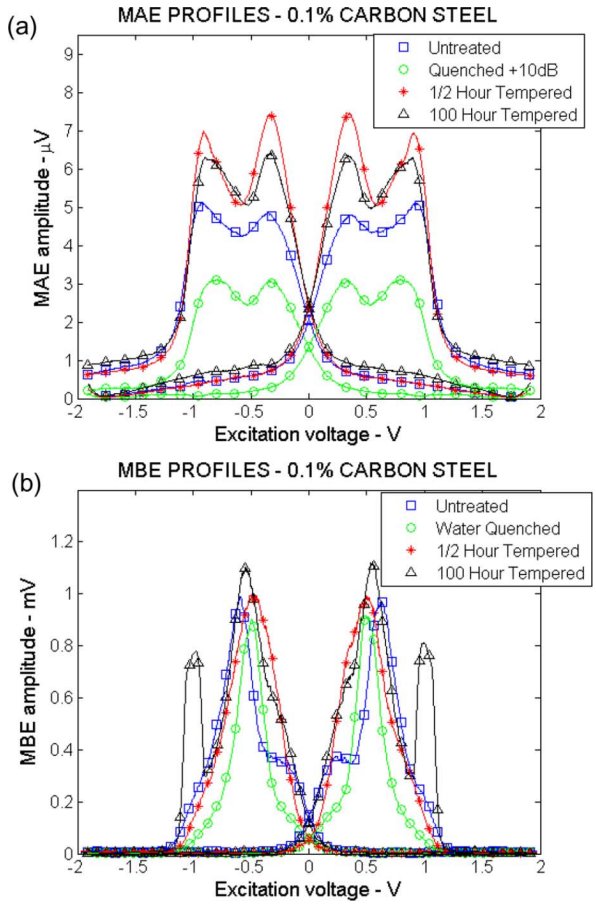

Fig. 3. (a) MAE and (b) MBE profiles for four pieces of 0.1% carbon steel using 2 Hz excitation.

tempered sample. MBE activity continues to increase with significant side lobes appearing in the plot for 100-h tempering.

IV. Case Depth Measurement for En36 Gear Steel

In this section, the comparative strengths of MAE and MBE for case depth measurement in En36 gear steel are studied. The effects of sample geometry and excitation signal frequency on test results are also examined. Samples b1–b5 are used in the tests.

A. Case Depth Measurement

MAE and MBE measurements were made for En36 bar samples with differing case depths at excitation frequencies of 1 Hz–0 Hz in 1 Hz increments, with data also acquired at 0.2 Hz for MBE only. Fig. 4 shows a selection of MBE and MAE profiles generated from the test data. The 0.2 Hz [Fig. 4(a)] and 1 Hz [Fig. 4(c)) MBE profiles and the 1 Hz (Fig. 4(b)] MAE profiles exhibit a monotonic reduction in amplitude as case depth increases. This is as expected; as the depth of the case hardened layer increases, the amount of hardened material within the measurement depth of the techniques increases. The hardened material exhibits less Barkhausen activity than the soft core, so the overall amplitude reduces. Although the overall level of MBE and MAE activity reduces with an increase in case depth, a more detailed analysis of the profiles shows some discrepancies between the two techniques.

It can be seen from the plots that the untreated sample generates a much higher level of both MBE and MAE (in the plots MBE is attenuated by 25 dB and MAE by 20 dB). As the untreated sample is the same microstructural state as the core of the case hardened samples, we can conclude that we are not receiving a large signal from the core of the material in the case hardened samples for either technique. Although this is a predictable outcome for MBE with its low measurement depth, it contradicts the accepted view that MAE has a much greater measurement depth than MBE and suggests that for this particular test, the MAE signal from the soft core is considerably attenuated.

Considering the macroscopic behavior of the material, a possible contributing factor for the decrease in MAE activity for the case hardened samples in comparison with the untreated sample is the reduction in the rate of change of magnetization in the core of the treated sample, due to a decrease in induction swing from material hardening. However, the excitation frequency is low, skin effects are negligible and the untreated core has a much higher permeability than the surface layer, consequently flux density in the core should not be greatly reduced in comparison with the untreated sample.

Fig. 5 shows some typical MAE [Fig. 5(a)] and MBE [Fig. 5(b)] profiles. Two peaks are identifiable in the MBE profile, whereas three peaks are identifiable in the MAE profile. As the soft core experiences maximum domain wall motion at lower field intensity than the surface layer, MBE peak 1 represents domain activity within the soft core and MBE peak 2 represents domain activity within the case hardened layer. Examination of Fig. 4 shows that MBE peak 1 can only be seen in Fig. 4(a); this is due to the lower high-pass MBE selection filter characteristic that is used in conjunction with 0.2 Hz excitation allowing deeper MBE sources to be measured. It can be seen from Fig. 4(a) that the relative amplitude of MBE peak 1 reduces as case depth increases and for 1.00 mm and 1.35 mm case depths, the soft core is no longer within the MBE measurement range and peak 1 is no longer apparent.

If we apply a similar analysis to the MAE profiles, MAE peak 2 should correspond to domain activity within the soft core and MAE peak 3 to domain activity within the case hardened

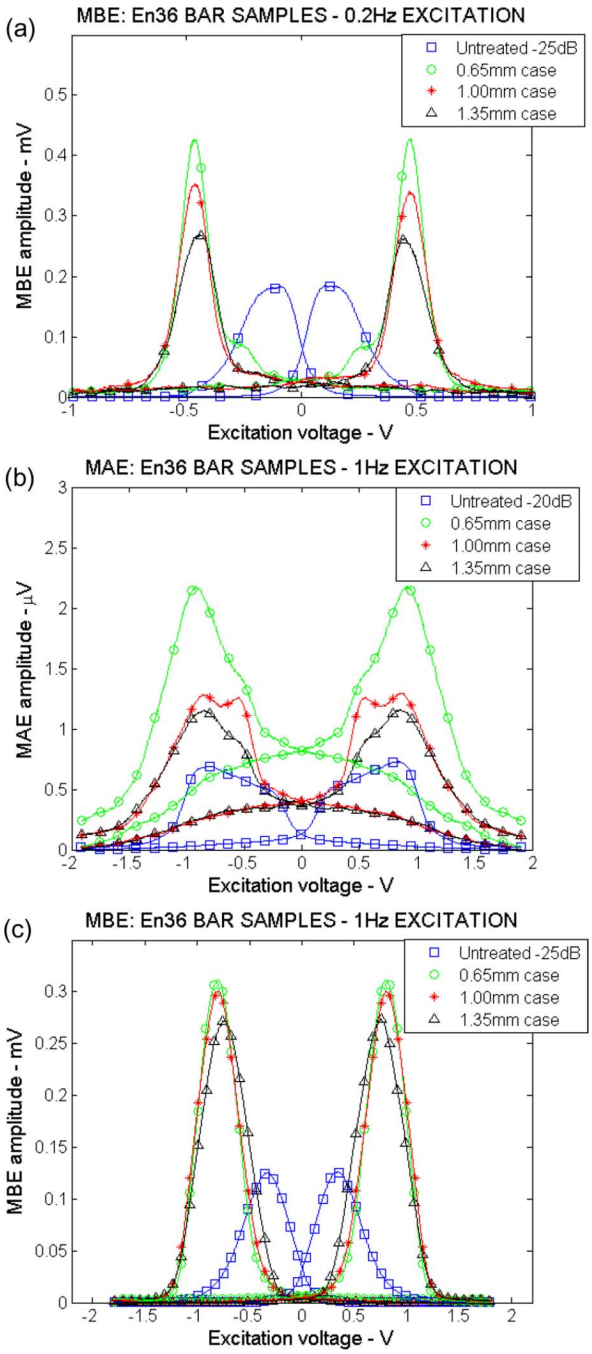

Fig. 4. Profiles for untreated and case hardened En36 samples for: a) MBE with 0.2 Hz excitation, b) MAE with 1 Hz excitation, and c) MBE with 1 Hz excitation.

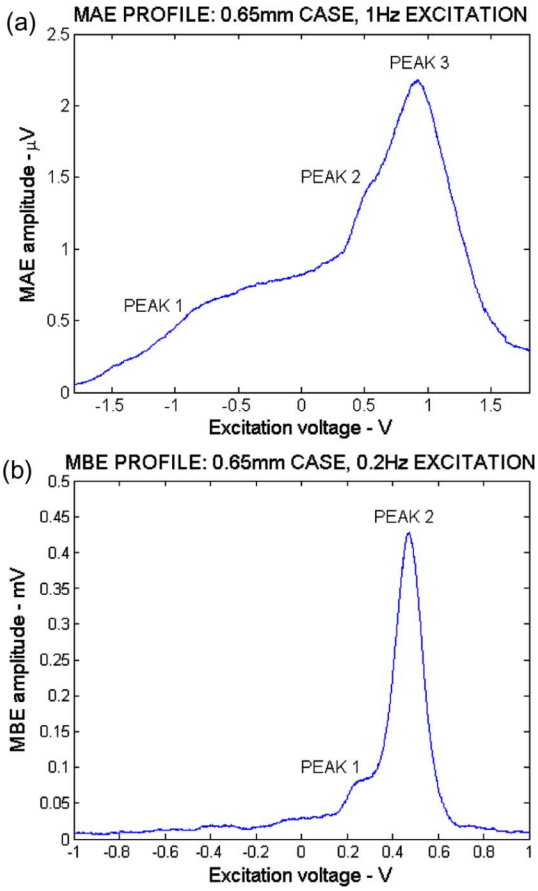

Fig. 5. Typical En36 MAE profile with peaks labeled, b) typical En36 MBE profile with peaks labeled.

layer, MAE peak 1 corresponds to low-level Barkhausen activity during the demagnetizing part of the hysteresis cycle, which can also be observed to some extent in the MBE plot. So we would expect a decrease in the relative amplitude of MAE peak 2 with an increase in case depth. However, this type of analysis does not hold true. Examination of Fig. 4(b) shows that the relative amplitude of MAE peak 2 actually increases with an increase in case depth.

One possible implication of this is that MAE peak 2 corresponds to domain activity within the case hardened layer, with peak 3 corresponding to activity within the soft core. This can be explained thus: If MAE can be measured throughout the volume of the sample with low frequency excitation; the field intensity will vary at different positions within that sample throughout the excitation cycle. For example, if we use 2 Hz, 2 V excitation with a 1 mm case depth sample, the soft material at around 1.2 mm may undergo maximum domain wall activity at ∼0.5 V, whereas material at a depth of 5 mm may undergo maximum domain wall activity at ∼1.5 V (field intensity always diminishes with depth), so we have a signal from the soft core throughout the excitation cycle, potentially masking the signal from the case hardened layer. The MAE peak 3 position is simply the point in the excitation cycle where the majority of the material in the sample is undergoing maximum domain wall activity, thus explaining the broadening of the MAE signal in comparison with MBE. Peak 2 corresponds to activity within the case hardened layer, partially masked by the signal from the soft core. The fact that there is a large amplitude difference between the untreated and case hardened samples indicates that a considerable level of flow around [6] is being exhibited in this narrow sample.

B. Influence of Sample Geometry

Fig. 6 shows MAE and MBE profiles for two samples:

- Sample b4: 1.00 mm case hardened En36 bar;
- Sample c1: 1.00 mm case hardened En36 block.

The samples are both case hardened to a depth of 1.00 mm, but have differing dimensions (see Table I). The MAE and MAE

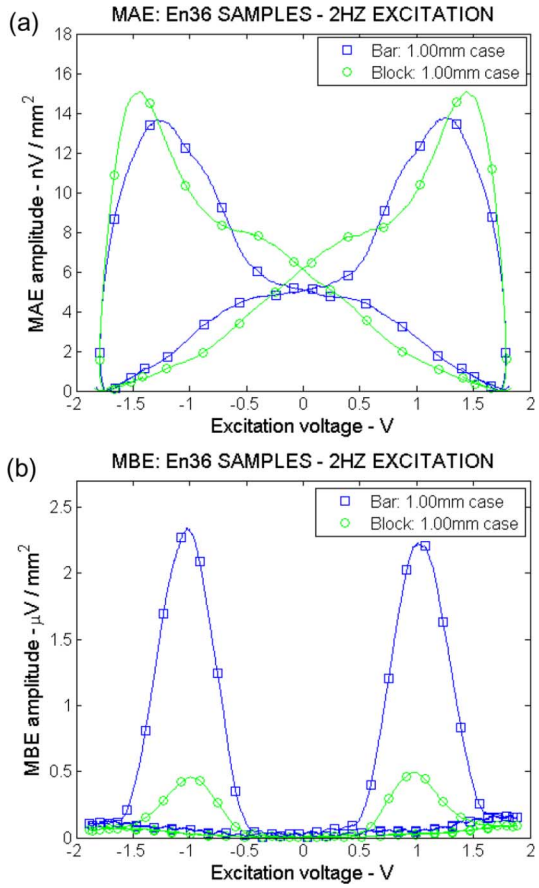

Fig. 6. (a) MAE profiles for 1 mm case hardened samples with different dimensions, b) MBE profiles for 1 mm case hardened samples with different dimensions. MAE and MBE profiles normalized to cross-sectional area of samples.

amplitudes have been normalized with respect to the cross-sectional area of the samples. The MBE profile in Fig. 6(b) shows an increase in amplitude for the bar sample, due to an intensification of the induced magnetic flux density as the excitation field is channeled into a sample with a reduced width (i.e., the flux lines cannot spread out as much in the narrower sample). However, for the MAE profiles shown in Fig. 6(a), the overall amplitudes for the bar and block samples is much closer than for MBE, indicating that MAE amplitude is, to some degree, proportional to the cross-sectional area of the material under inspection.

This result highlights the large influence that sample geometry has over MAE and MBE results. It can be seen from Fig. 6(a) that the position of MAE peak 3 is at a greater excitation voltage for the block sample due to the higher field strength needed to magnetize the larger sample. The increase in MAE signal strength for the block sample could be due to increased penetration of the applied field in the block sample due to a lessening of the flux flow around [6] corresponding to the increased width in comparison to the bar sample. If this is the case, the increased activity at around 0.4 V corresponds to increased activity in the soft core, due to increased penetration. As MBE is a near-surface inspection technique, the increased penetration in the block sample is not apparent from the result and the overriding influence is from the localized increase in flux density between the core poles at the inspected surface of the bar sample.

C. *Influence of Excitation Frequency Variation on Barkhausen Profiles*

Fig. 7(a) shows MAE and MAE peak positions with respect to excitation voltage maximum. The peak positions are represented in terms of the phase shift between the excitation voltage maxima and signal maxima (MAE peak 3 and MBE peak 2). For example, 0° corresponds to the signal maximum coinciding with the excitation voltage maximum; −90° corresponds to a phase shift of 1/4 excitation cycle between excitation and signal maxima. As the excitation signal is measured as the voltage applied to the power amplifier, as shown in Fig. 1, there is some phase difference between measured excitation voltage and applied field, but as this exists for both MAE and MBE, the plots are comparable. Plots are shown for sample b4; 1 mm case hardened En36 bar only, but all case hardened En36 bar samples produce similar plots.

The increase in excitation frequency causes a change in the magnetic flux in the sample in terms of both phase and distribution [6], [7]. As excitation frequency is increased there is a greater phase variation in the induced field throughout the volume of the sample. The distribution of the field is modified due to the skin effect and more importantly an increase in flow around and the associated decrease in field penetration. So for higher excitation frequencies, we have a greater concentration of the flux within the surface layer of the sample, coupled with a greater variation of phases throughout the sample volume. These changes in flux phase and distribution will have a much greater impact on MAE than MBE, due to the localised measurement characteristics of MBE. This can be seen in Fig. 7(a), where the difference between the plots for MAE and MBE increases with increasing excitation frequency, with MAE showing the greatest variation in phase shift for the frequencies used in the tests.

Fig. 7 shows MAE and MBE profiles for sample b4; 1 mm case hardened En36 bar, for excitation frequencies of 1 Hz, 5 Hz, and 10 Hz. Profiles for half an excitation cycle are plotted against phase, relative to excitation voltage maxima, with 0° corresponding to the maximum excitation voltage. A broadening of the major MAE peak with an increase in excitation frequency can be seen in Fig. 7(a), while the MBE peak is relatively narrow. This has been widely reported [6]–[8] and is thought to be due to increased phase variations throughout the sample as excitation frequency is increased. As MBE operates over a much smaller volume of material, the broadening effect is not as pronounced for MBE [Fig. 7(c)]. The increase in excitation frequency also causes a blurring of MAE profile features, due to increased phase variations within the volume of the sample, however, two signal peaks can still be discerned in the 10 Hz profile.

V. Conclusion

In this paper, comparative MAE and MBE results have been put forward for the quantification of heat treatment in 0.1% carbon steel and case hardening in En36 gear steel. The generation of the signal profile with respect to excitation voltage has been chosen as the primary signal analysis tool. MBE results are as would be expected and broadly agree with earlier tests carried out by Moorthy *et al.* [1], [2], and an overall reduction in signal amplitude can be seen for an increase in case depth for both techniques.

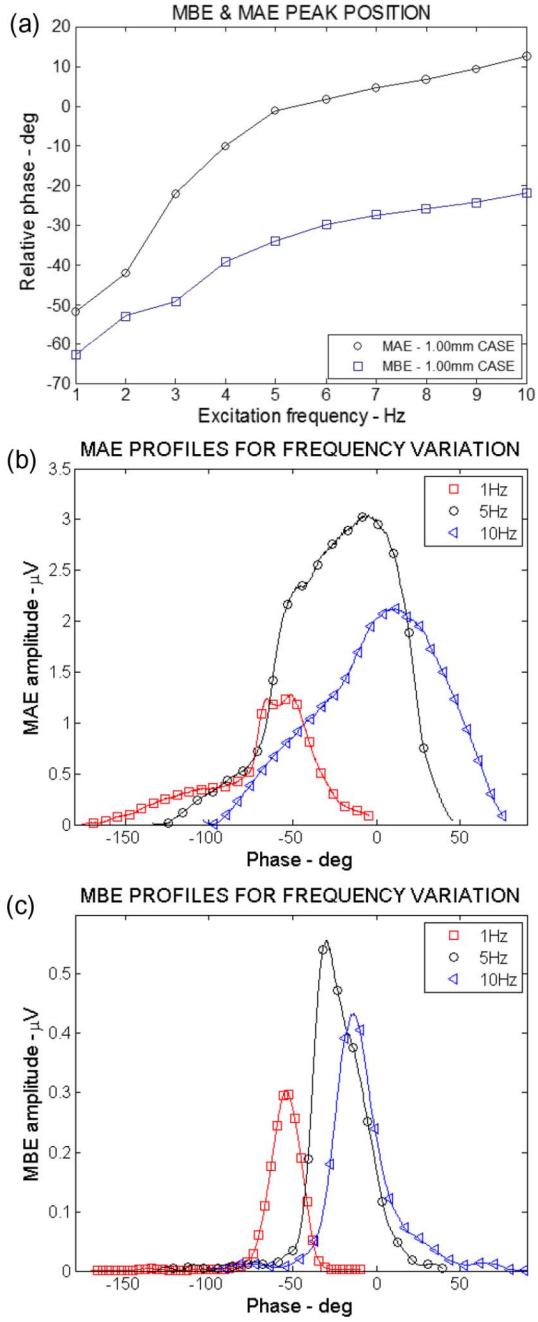

Fig. 7. a) MAE and MBE maxima relative phase with respect to excitation voltage maxima for sample b4, b) MAE profiles for sample b4 for 1 Hz, 5 Hz, and 10 Hz excitation, and c) MBE profiles for sample b4 for 1 Hz, 5 Hz, and 10 Hz excitation.

MAE can obtain wide or multiple peaks at higher frequencies than MBE signals for samples with different case depths. This indicates the possibility of deeper stress profile measurement using MAE than using MBE, but the correlation between MAE activity at different depths and profile features needs further study for the evaluation of quantitative information. The measurement depth of MAE is usually presumed to be proportional to the skin depth in the material under inspection, but the test results offered in this paper show that this assumption is oversimplified, as the overall amplitude for the untreated En36 sample is much greater than the overall amplitude for the case hardened En36 samples, it can be concluded that relatively little MAE is being received from the soft core of the case hardened samples. Some reduction in sensitivity as case depth increases is also observable. The most convincing explanation for this is that the narrow En36 bar samples experience a considerable amount of flow around; the tendency for the flux in a ferromagnetic material to concentrate in the surface layer en route to the bottom side of the sample, rather than traversing the bulk of the sample. Thus, the penetration of the soft core is more limited than a simple skin depth calculation would imply. Further work will investigate the quantification of residual stress gradients from treatments such as laser peening using a combination of MAE and MBE.

REFERENCES

[1] V. Moorthy, B. A. Shaw, and P. Hopkins, "Surface and subsurface stress evaluation in case-carburised steel using high and low frequency magnetic Barkhausen emission measurements," *J. Magn. Magn. Mater.*, vol. 299, no. 2, pp. 362–375, Apr. 2006.

[2] V. Moorthy, B. A. Shaw, and J. T. Evans, "Evaluation of tempering induced changes in the hardness profile of case-carburised EN36 steel using magnetic Barkhausen noise analysis," *NDT & E Int.*, vol. 36, no. 1, pp. 43–49, Jan. 2003.

[3] D. J. Buttle, C. B. Scruby, G. A. D. Briggs, and J. P. Jakubovics, "The measurement of stress in steels of varying microstructure by magnetoacoustic and Barkhausen emission," *Proc. R. Soc. Lond. A*, vol. 414, pp. 469–497, 1987.

[4] D. O'Sullivan, M. Cotterell, S. Cassidy, D. A. Tanner, and I. Mészáros, "Magneto-acoustic emission for the characterisation of ferritic stainless steel microstructural state," *J. Magn. Magn. Mater.*, vol. 271, no. 2–3, pp. 381–389, May 2004.

[5] S. B. Tochilin, J. P. Jakubovics, and G. A. D. Briggs, "Use of magnetoacoustic emission for studying stress in industrial components," *IEEE Trans. Magn.*, vol. 31, no. 6, pp. 4163–4165, Nov. 1995.

[6] M. Augustyniak, B. Augustyniak, M. Sablik, and W. Sadowski, "The finite element method simulation of the space and time distribution and frequency dependence of the magnetic field and MAE," *IEEE Trans. Magn.*, vol. 43, no. 6, pp. 2758–2760, Jun. 2007.

[7] M. Augustyniak, B. Augustyniak, L. Piotrowski, M. Chmielewski, and W. Sadowski, "Evaluation by means of magneto-acoustic emission and Barkhausen effect of time and space distribution of magnetic flux density in ferromagnetic plate magnetized by a C-core," *J. Magn. Magn. Mater.*, vol. 304, no. 2, pp. e552–e554, Sep. 2006.

[8] H. C. Kim and C. G. Kim, "Effect of magnetising frequency and stress on magneto-acoustic emission from 3% Si-Fe crystals," *J. Phys. D: Appl. Phys.*, vol. 22, no. 1, pp. 192–198, 1989.

[9] A. Dhar and D. L. Atherton, "Magnetizing frequency dependence of magneto-acoustic emission in pipeline steel," *IEEE Trans. Magn.*, vol. 28, no. 2, pp. 1003–1007, Mar. 1992.

[10] C. C. H. Lo, C. B. Scruby, and G. D. W. Smith, "Dependences of magnetic Barkhausen emission and magnetoacoustic emission on the microstructure of pearlitic steel," *Philos. Mag.*, vol. 84, no. 18, pp. 1821–1839, 2004.